

# Theory of anisotropic s-wave superconductivity with point-node like gap minima: analysis of (Y,Lu)Ni<sub>2</sub>B<sub>2</sub>C

Hiroshi KONTANI

Department of Physics, Saitama University, 255 Shimo-Okubo, Saitama-city, 338-8570, Japan.  
(September 14, 2018)

Recent intensive experimental studies revealed that (Y,Lu)Ni<sub>2</sub>B<sub>2</sub>C is an anisotropic s-wave superconductor. In addition, its gap function possesses deep point minima, whose ratio of the gap anisotropy is more than 10. On the theoretical side, however, it is nontrivial to understand the origin of such a peculiar superconductivity. In the present paper, we propose a mechanism of the s-wave superconductivity with deep gap minima, based on the theoretical model where strong electron-phonon coupling as well as the moderate magnetic fluctuations coexist. By analyzing the strong coupling Eliashberg equation, we find that s-wave superconducting gap function owing to the electron-phonon coupling becomes highly anisotropic as the magnetic fluctuations increases. The set of model parameters for realizing the strong gap anisotropy in the present model will be appropriate for (Y,Lu)Ni<sub>2</sub>B<sub>2</sub>C. According to the present mechanism, (groups of) pair of gap minima appear at points on the Fermi surface which are connected by the nesting vector  $\mathbf{Q}$ , in both cases of s-wave superconductors and non s-wave ones. We briefly discuss other superconductors with highly anisotropic gap function, e.g., PrOs<sub>4</sub>Sb<sub>12</sub> and Na<sub>0.33</sub>CoO<sub>2</sub>.

PACS numbers: 74.20.-z, 74.20.Fg, 74.40.+k

## I. INTRODUCTION

### A. superconductivity in RENi<sub>2</sub>B<sub>2</sub>C

Since the boron-carbide superconductors RENi<sub>2</sub>B<sub>2</sub>C (RE=Lu, Y, Tm, Er, Ho, Dy) was discovered about a decade ago [1], various experimental and theoretical studies have been devoted to determine the symmetry or the mechanism of the superconductivity. The crystal structure is body-centered tetragonal, consists of RE-C layers separated by Ni<sub>2</sub>B<sub>2</sub> sheets. Among them, LuNi<sub>2</sub>B<sub>2</sub>C and YNi<sub>2</sub>B<sub>2</sub>C show relatively high  $T_c$ , 16.5K and 15.5K, respectively. They are non-magnetic metals till very low temperatures. On the other hand, in superconducting Er and Ho compounds, *f*-electrons in Er and Ho show incommensurate magnetic long range orders with  $\mathbf{Q}_m \approx 2\pi(0.55/a, 0, 0)$ , where  $a$  is the lattice spacing [2,3].

Various experimental results revealed that LuNi<sub>2</sub>B<sub>2</sub>C and YNi<sub>2</sub>B<sub>2</sub>C are s-wave superconductors, whose superconducting (SC) gap functions are highly anisotropic. For example, the specific heat measurement in YNi<sub>2</sub>B<sub>2</sub>C below  $T_c$  tells that the SC gap in these compounds changes from a gap-less type to a full-gap one, by replacing Ni with Pt by 20% [4]. This result suggests that a s-wave superconductivity with deep point minima occurs in a pure compound, and its anisotropy is smeared out by impurities. Later, Izawa et al. measured the *c*-axis thermal conductivity of YNi<sub>2</sub>B<sub>2</sub>C in  $\mathbf{H}$  rotated in various directions, and found that deep point minima in SC gap exist along [100] and [010] directions [5]. The estimated ratio of the anisotropy of the SC gap will be more than 10. Recently, Watanabe et al. confirmed the point-node

like SC gap function along [100] and [010] directions by the ultrasonic attenuation measurement [6].

On the theoretical side, however, the origin of such a highly anisotropic s-wave SC gap has not been understood until now. It cannot be reproduced by solving an Eliashberg equation even if one assume a highly anisotropic dispersion for conduction electrons and/or anisotropic electron-phonon (e-p) interactions. Thus, a reasonable theoretical model for the anisotropic s-wave SC gap with deep point minima, whose ratio of anisotropy is more than 10, is highly demanded for understanding the superconductivity in (Y,Lu)Ni<sub>2</sub>B<sub>2</sub>C.

In the present paper, we propose a mechanism of an anisotropic s-wave superconductivity with deep gap minima, in a system where strong e-p coupling and moderate antiferromagnetic (AF) fluctuations coexist. By solving the strong coupling Eliashberg equation, we succeed in deriving a s-wave SC gap with deep point minima, whose ratio of anisotropy is more than 10, for a wider range of model parameters. The point-node like SC gap in (Y,Lu)Ni<sub>2</sub>B<sub>2</sub>C observed experimentally is reasonably explained by the present theory. The proposed mechanism of making deep gap minima due to the magnetic fluctuations is simple and general, so it will also be realized in various superconductors, including the unconventional superconductors. We study the case of the p-wave SC system in Appendix.

By various experimental and theoretical studies for (Y,Lu)Ni<sub>2</sub>B<sub>2</sub>C, it is confirmed that both (i) *strong e-p couplings* and (ii) *prominent AF fluctuations due to the nesting of the Fermi surface (FS)* coexist in these compounds. Here, we explain the experimental and theoretical evidences of (i) and (ii) in more detail.

## B. evidence for AF fluctuations

NMR studies for (Y,Lu)Ni<sub>2</sub>B<sub>2</sub>C have been performed by several authors [7,8]. The spin-lattice relaxation ratio  $1/T_1$  of <sup>11</sup>B and that of <sup>89</sup>Y do not show Hebel-Slichter peaks. In the normal state, on the other hand,  $1/T_1T$  of <sup>11</sup>B increases monotonously as temperature decreases, which suggests the enhancement of the AF fluctuations at lower temperatures. According to the spin fluctuation theory like the SCR theory [9],  $1/T_1T \propto \chi_Q^{2-d/2}$ , where  $d$  is the dimension of the system and  $\chi_Q$  is the staggered susceptibility. In nearly AF metals,  $\chi_Q$  shows the Curie Weiss temperature dependence. The observed  $1/T_1T$  of <sup>11</sup>B can be fitted well by the above expression both for  $d=2$  and 3.

The strong AF fluctuations in (Y,Lu)Ni<sub>2</sub>B<sub>2</sub>C observed by NMR are expected to originate from the nesting of the FS: According to the LDA band calculations for LuNi<sub>2</sub>B<sub>2</sub>C [10–13], the FS possesses a nesting feature whose nesting vector is  $\mathbf{Q} \approx 2\pi(0.5/a, 0, 2\pi(0, 0.5/a)$ . The generalized susceptibility  $\chi_{\mathbf{q}}^0(0)$  derived from the band structure given by the LDA study shows a peak at  $\mathbf{q} \sim \mathbf{Q}$  [10], which means that the RPA-type magnetic susceptibility,  $\chi_{\mathbf{q}}(0) = \chi_{\mathbf{q}}^0(0)/(1 - U\chi_{\mathbf{q}}^0(0))$ , has a sharp maximum at  $\mathbf{q} \sim \mathbf{Q}$ .

Another evidence of the nesting for  $\mathbf{q} \sim \mathbf{Q}$  is the magnetic order of *f*-electrons in Er and Ho compounds, whose ordering vector is  $\mathbf{Q}_m \approx 2\pi(0.55/a, 0, 0)$ . This ordering is given by the RKKY interaction between *f*-electrons via the susceptibility of conduction electrons. Because all the band structures for RENi<sub>2</sub>B<sub>2</sub>C will be similar owing to the local nature of *f*-orbitals of RE,  $\chi_{\mathbf{q}}(0)$  in (Y,Lu)Ni<sub>2</sub>B<sub>2</sub>C is expected to take the maximum value around  $\mathbf{q} \approx \mathbf{Q}_m \approx \mathbf{Q}$ .

## C. evidence for strong e-p coupling

The density of states (DOS) at the Fermi energy in RENi<sub>2</sub>B<sub>2</sub>C obtained by the band calculation is  $4.5 \sim 4.8(\text{eV cell})^{-1}$  [11–13]. Because a cell contains two Ni atoms, the DOS per Ni is  $2.25 \sim 2.4\text{eV}^{-1}$ . This value of the DOS is much larger than that for high- $T_c$  cuprates, which is about  $\sim 1.3(\text{eV cell})^{-1}$  by the band calculation for La<sub>2</sub>CuO<sub>4</sub>, where a cell contains one Cu atom.

Such a huge DOS in RENi<sub>2</sub>B<sub>2</sub>C suggests the strong e-p coupling. In addition, the light weight of B atom means the large frequency of the phonon mode,  $\omega_{\text{ph}}$ . In fact,  $\omega_{\text{ph}} \sim 300\text{K}$  is expected in these compounds [13]. The dimensionless e-p coupling constant  $\lambda$  (or mass enhancement factor due to e-p interaction) is defined as  $\lambda \equiv m^*/m_{\text{band}} - 1$ , where  $m^*$  is the effective mass of an electron. Its value can be estimated by the temperature dependence of resistivity  $\rho$  using the Bloch-Gruneisen transport theory. The experimental value  $0.4\mu\Omega\text{cm}/\text{K}$  in LuNi<sub>2</sub>B<sub>2</sub>C leads to  $\lambda \sim 2.6$ , although it might be too

overestimated [11]. In addition, we stress that the prominent softening of the phonon dispersion at  $\mathbf{k}_{\text{obs}} \sim \mathbf{Q}$  is observed by neutron diffraction experiments [19]. This result strongly suggests the strong e-p coupling as well as the nesting of the FS with  $\mathbf{k}_{\text{obs}} \sim \mathbf{Q}$ . Thus, the observed Kohn anomaly ensures the main character of the electronic properties in (Y,Lu)Ni<sub>2</sub>B<sub>2</sub>C.

The estimations of the value of  $\lambda$  using the thermodynamic measurements have been tried by many authors on the basis of the strong coupling Eliashberg equation. References [14] and [15] concluded that  $\lambda = 1 \sim 1.2$ . On the other hand,  $\lambda = 0.5 \sim 0.8$  was deduced using the scanning tunnelling spectroscopy [16]. In addition, a moderate momentum dependence of (or FS dependence of)  $\lambda$  was inferred by several authors: Reference [17] explained the experimental upper critical field ( $H_{c2}$ ) by assuming a two-band model with different  $\lambda$ 's ( $\lambda_{\text{max}} = 0.8$  and  $\lambda_{\text{min}} = 0.3$ ). Later, more isotropic  $\lambda$  was inferred by ref. [15]. More recently, Yamauchi et al. studied the mass enhancement factor  $\lambda = m_{\text{dHvA}}/m_{\text{band}} - 1$ , where  $m_{\text{band}}$  in the band mass given by the LDA study, and  $m_{\text{dHvA}}$  is the cyclotron mass measured by the dHvA study, by assuming that the mass enhancement is caused only by e-p couplings [18]. The obtained  $\lambda$ 's are  $0.1 \sim 0.76$  depending on the portion of FS's.

However, previous works based on the strong coupling study could not reproduce the strongly anisotropic s-wave SC gap as observed in (Y,Lu)Ni<sub>2</sub>B<sub>2</sub>C, even if one assume a multi-band model with very different  $\lambda$ 's. In the present paper, we show the importance of the AF fluctuations to reproduce the deep point minima of the gap function found in (Y,Lu)Ni<sub>2</sub>B<sub>2</sub>C.

## D. s-wave or d-wave: theoretical viewpoint

The existence of the prominent AF fluctuations in RENi<sub>2</sub>B<sub>2</sub>C suggest the possibility of the d-wave SC state, like in high- $T_c$  superconductors. Fukazawa et al. performed the third order perturbation analysis with respect to  $U$  in a two-dimensional tight-binding Hubbard model for (Y,Lu)Ni<sub>2</sub>B<sub>2</sub>C, by neglecting the e-p couplings [28]. By solving the Eliashberg equation, they found that  $T_c \sim 15\text{K}$  for d-wave symmetry is realized by choosing a reasonable strength of  $U$ . However, the obtained  $T_c$  might be overestimated because d-wave  $T_c$  is relatively low in the case of 3D systems in general. In fact, the FS of RENi<sub>2</sub>B<sub>2</sub>C given by band calculations possesses a three-dimensional (3D) structure, rather than a two-dimensional one. Experimentally, the anisotropy of the resistivity as well as that of  $H_{c2}$  are small. In this sense, this compound is a three-dimensional superconductor.

Next, we crudely estimate the s-wave  $T_c$  due to the strong e-p coupling in RENi<sub>2</sub>B<sub>2</sub>C. By taking strong coupling effects into account, following BCS-McMillan [21] type expression for  $T_c$  valid for  $\lambda \sim O(1)$  would be obtained:

$$T_c = (\omega_{\text{ph}}/1.2) \exp(-1/(\lambda^* - \mu^*)), \quad (1)$$

where  $\lambda^* \equiv \lambda/(1 + \lambda)$  and  $\mu^*$  is the Morel-Anderson pseudo-potential, which represents the reduction of  $T_c$  owing to the pair-breaking effect by the Coulomb interaction. By putting  $\lambda = 1.5$ ,  $\omega_{\text{ph}} = 300\text{K}$ , and  $\mu^* = 0.15$  (a typical value) in eq.(1), we obtain  $T_c = 27\text{K}$ . If we put  $\lambda = 1.0$  instead,  $T_c = 14\text{K}$  is obtained.

In the following sections, we study the s-wave superconductivity caused by the e-p coupling, under the influence of prominent AF fluctuations. We propose an effective model for (Y,Lu)Ni<sub>2</sub>B<sub>2</sub>C which reflect their characteristic properties well. By solving the strong coupling Eliashberg equation, we succeed in deriving the s-wave SC gap function with deep gap minima. The proposed mechanism of the strongly anisotropic SC gap, which is developed to explain the superconductivity in (Y,Lu)Ni<sub>2</sub>B<sub>2</sub>C, might be applicable to several unconventional superconductors found recently.

## II. THEORETICAL MODEL

### A. model with e-p coupling and AF fluctuations

In this section, we explain the theoretical model used in the present work. In the present paper, we study the mechanism of the anisotropic s-wave superconductivity based on the simplified two-dimensional model under the influence of the magnetic fluctuations, which have not been studied previously. The proposed mechanism is expected to occur in real compounds which have complex three-dimensional FS's.

For the simplicity of the analysis, we assume a two dimensional isotropic Fermi surface as shown in Fig.1(a). In addition, the density of states (DOS) at the Fermi level,  $N(0)$ , is assumed to be isotropic. Hereafter, we put  $k_F = 2.5$ , which corresponds to  $n = 0.50$  (quarter filling) if the area of the Brillouin zone is  $(2\pi)^2$  (square lattice).

Next, we introduce the electron-electron interaction terms owing to the e-p interaction and the AF fluctuations. The latter originates from the (on-site) Coulomb interaction and the nesting of the FS. First, we represent the interaction between electrons due to phonons,  $V^{\text{ph}}(\omega)$ . In the case of the Einstein-type phonon,

$$V^{\text{ph}}(\omega + i\delta) = \frac{g\omega_{\text{ph}}}{2} \frac{2\omega_{\text{ph}}}{(\omega^2 - \omega_{\text{ph}}^2) + i\omega\delta}, \quad (2)$$

where  $\omega_{\text{ph}}$  is the frequency of the Einstein phonon.  $g$  has a dimension of energy, and  $\lambda \equiv gN(0)$  gives the dimensionless coupling constant due to phonons. In (Y,Lu)Ni<sub>2</sub>B<sub>2</sub>C,  $\omega_{\text{ph}} \sim 300\text{K}$  and  $gN(0) \sim 1$  is expected as mentioned in the previous section.

We also introduce the interaction between electrons due to AF fluctuations,  $V_{\mathbf{q}}^{\text{AF}}(\omega)$ . In a Hubbard model with on-site interaction,  $U$ , it is given by  $\frac{3U^2}{2}\chi_{\mathbf{q}}(\omega)$

within the RPA or fluctuation-exchange (FLEX) type approximation [22]. In the RPA or FLEX approximation, the magnetic susceptibility  $\chi_{\mathbf{q}}(\omega)$  is given by  $\chi_{\mathbf{q}}(\omega) = \chi_{\mathbf{q}}^0(\omega)/(1 - U\chi_{\mathbf{q}}^0(\omega))$ , where  $\chi_{\mathbf{q}}^0(\omega)$  is the irreducible susceptibility. Here, we assume the following effective  $V_{\mathbf{q}}^{\text{AF}}$  whose validity is assured in a lower energy region:

$$V_{\mathbf{q}}^{\text{AF}}(\omega + i\delta) = \frac{a}{1 + \xi_{\text{AF}}^2 |\mathbf{Q} - \mathbf{q}|^2 - i\omega/\omega_{\text{sf}}} \quad \text{model 1}, \quad (3)$$

$$= \frac{2a}{(1 + \xi_{\text{AF}}^2 |\mathbf{Q} - \mathbf{q}|^2)^2 - i\omega/\omega_{\text{sf}}} \quad \text{model 2}, \quad (4)$$

where  $\mathbf{Q}$  is the nesting vector where  $\chi_{\mathbf{q}=\mathbf{Q}}(0)$  takes the maximum value,  $\xi_{\text{AF}}$  is the AF correlation length, and  $\omega_{\text{sf}}$  represents the energy scale of the AF fluctuations. In both models,  $a$  has a dimension of energy, so  $aN(0)$  represents the dimensionless coupling constant for AF fluctuations.

The model 1 is derived directly from  $\chi_{\mathbf{q}}(\omega)$  within the RPA or FLEX approximation,  $\chi_{\mathbf{q}}(\omega) = \chi_{\mathbf{q}}^0(\omega)/(1 - U\chi_{\mathbf{q}}^0(\omega))$ , by expanding  $U\chi_{\mathbf{q}}^0(\omega)$  as  $U\chi_{\mathbf{Q}}^0(0) + \alpha_S \xi_{\text{AF}}^2 |\mathbf{Q} - \mathbf{q}|^2 - i\alpha_S \omega/\omega_{\text{sf}} + O(|\mathbf{Q} - \mathbf{q}|^4, \omega^2)$ , where  $\alpha_S \equiv 1 - U\chi_{\mathbf{Q}}(0) \ll 1$  is the Stoner factor. Then,  $a$  is given by  $\frac{3U^2}{2}\chi_{\mathbf{Q}}(0)$ . Thus, model 1 is has a correct functional form when  $|\mathbf{q} - \mathbf{Q}| \ll \xi_{\text{AF}}^{-1}$  and  $\omega \ll \omega_{\text{sf}}$ . The model 1 had been studied intensively by Monthoux, Pines and their collaborators in the study of high- $T_c$  superconductors [23]. Within the SCR theory [9] or FLEX-type approximation [22],  $\xi_{\text{AF}}^2 \propto T^{-1}$  and  $a \propto \omega_{\text{sf}}^{-1} \propto \xi_{\text{AF}}^2$ , which are observed experimentally in various high- $T_c$  cuprates. Especially,  $\omega_{\text{sf}} > T$  ( $< T$ ) in over-doped (under-doped) cuprates above the pseudo-gap temperatures, which is well reproduced by the FLEX approximation [24]. Apparently,  $\omega_{\text{sf}}$  becomes small in the close vicinity of the magnetic quantum critical point (QCP).

However, the model 1 might be unrealistic for  $|\mathbf{q} - \mathbf{Q}| \gg \xi_{\text{AF}}^{-1}$  in that it has a lorenzian form with respect to  $|\mathbf{q} - \mathbf{Q}|$ , which decays too slow. Instead of introducing a cutoff momentum  $q_c$  in the model 1, we introduce the model 2 which decays faster than lorenzian when  $|\mathbf{q} - \mathbf{Q}| \gg \xi_{\text{AF}}^{-1}$ . The functional form of the model 2 will be justified if we assume the following expansion  $U\chi_{\mathbf{q}}^0(0) = U\chi_{\mathbf{Q}}^0(0) + 2\alpha_S \xi_{\text{AF}}^2 |\mathbf{Q} - \mathbf{q}|^2 + \alpha_S^2 \xi_{\text{AF}}^4 |\mathbf{Q} - \mathbf{q}|^4 + O(|\mathbf{Q} - \mathbf{q}|^6)$ , where we fixed the coefficient of the forth order term as  $\alpha_S^2 \xi_{\text{AF}}^4$ . As a matter of convenience, we put 2 in the numerator of eq.(4) to make the weights  $\int_{-\infty}^{\infty} d^1q V_{\mathbf{q}}^{\text{AF}}(0)$  for both models equivalent. In the present study, we treat  $a$ ,  $\xi_{\text{AF}}$  and  $\omega_{\text{sf}}$  as independent parameters both in model 1 and in model 2.

The momentum dependences of model 1 and 2 for  $\omega = 0$  are shown in Fig. 2, where  $x \equiv |\mathbf{q} - \mathbf{Q}|$ .  $x$ -dependences of model 2 and model 3 (gaussian), both of which decay faster than lorenzian, looks similar. Although model 1 have been studied intensively in the

study of high- $T_c$  superconductors [23], its supremacy is not apparent for the purpose of the present study. Note that a similar  $T_c$  for d-wave will be obtained by solving the Eliashberg equation in each models for the same parameters in  $V_{\mathbf{q}}^{\text{AF}}(\omega)$ . In later sections, we study both model 1 and model 2, and analyze the latter model mainly.

Finally, we point out that the isotropic FS used in the present study contradicts with the emergence of AF fluctuations, which should arise as a result of the nesting of the FS. This contradiction in the theoretical model will be discussed later. Although this simplification is unrealistic, it eliminates extrinsic complication in discussion and make the result clear. This simplification will not harm the generality of the the mechanism of the superconductivity with deep gap minima proposed in the present paper.

## B. origin of the deep SC gap minima

Here, we explain qualitatively about the origin of the s-wave SC gap with deep minima. In the weak coupling BCS theory, where SC order parameter  $\Delta_{\mathbf{k}}$  is treated as energy-independent, it will be allowed to replace eqs.(2) and (3) with  $-g\theta(\omega_{\text{ph}} - |\omega|)$  and  $V_{\mathbf{k}-\mathbf{p}}^{\text{AF}}(0) \cdot \theta(\omega_{\text{sf}} - |\omega|)$ , respectively [25]. As a result,  $T_c$  within the weak coupling BCS theory is given by the highest temperature for the non-trivial solution  $\Delta_{\mathbf{k}} \neq 0$  of

$$\Delta_{\mathbf{k}} = \sum_{\mathbf{p}} g \frac{\Delta_{\mathbf{p}}}{2E_{\mathbf{p}}} \tanh \left( \frac{E_{\mathbf{p}}}{2T} \right) \theta(\omega_{\text{ph}} - E_{\mathbf{p}}) - \sum_{\mathbf{p}} V_{\mathbf{k}-\mathbf{p}}^{\text{AF}}(0) \frac{\Delta_{\mathbf{p}}}{2E_{\mathbf{p}}} \tanh \left( \frac{E_{\mathbf{p}}}{2T} \right) \theta(\omega_{\text{sf}} - E_{\mathbf{p}}), \quad (5)$$

where a singlet pairing is assumed. In the above equation,  $E_{\mathbf{p}} \equiv \sqrt{(\epsilon_{\mathbf{p}} - \mu) + \Delta_{\mathbf{p}}^2}$ , where  $\epsilon_{\mathbf{p}}$  is the dispersion of the conduction election and  $\mu$  is the chemical potential. The minus sign of the second term of eq.(5) can be interpreted as reflecting that  $\langle \vec{s} \cdot \vec{s}' \rangle = -3/4$  for a singlet Cooper pair. In the absence of the AF fluctuations,  $T_c^0 = 1.13\omega_{\text{ph}} \exp(-1/\lambda)$  for s-wave superconductivity is obtained by eq.(5) when  $\lambda \equiv gN(0) \ll 1$  [25]. On the other hand, in the case of  $g = 0$ , the solution of eq.(5) is the  $d_{xy}$ -wave like owing to the second term of eq.(5),  $\Delta_{k_x, k_y} = -\Delta_{-k_x, k_y} = -\Delta_{k_x, -k_y} = \Delta_{-k_x, -k_y}$ , as shown in Fig. 1(d). On the other hand,  $d_{x^2-y^2}$ -type pairing is not favorable energetically when  $\mathbf{Q} \sim (2k_F, 0), (0, 2k_F)$ .

Here we consider the s-wave solution of the gap function  $\Delta_{\mathbf{k}}$  in eq.(5) owing to the strong e-p coupling. As the coupling constant for AF fluctuations,  $aN(0)$ , increases,  $\Delta_{\mathbf{k}}$  with s-wave symmetry will has minima at  $\theta_{\mathbf{k}} = n\pi/2$  ( $n$  being a integer) by reflecting the negative contribution from the second term of eq.(5); see Fig. 1(b). Because of the simplicity of the mechanism, this theory of the s-wave SC gap with deep minima due to AF fluctuations is expected to be general, independent of the fine shape of the

FS. However, one has to check that the s-wave  $T_c$ , which will be smaller than  $T_c^0$  ( $\equiv T_c$  without AF fluctuations), is larger than the d-wave  $T_c$  caused by AF fluctuations.

According to the present theory, each point minima is connected with others by  $\mathbf{Q}$ . In the case of  $|\mathbf{Q}| < 2k_F$ , eight point minima will emerge (instead of four), except for  $|\mathbf{Q}| = \sqrt{2}k_F$  (see fig.1 (c)). Except the number of point minima, the obtained results in the present study will qualitatively hold even if  $|\mathbf{Q}| < 2k_F$ . Here, we note that the position of the point gap minima is equivalent to that of “hot spots”, where the quasiparticle damping rate due to AF fluctuations take the (local) maximum value. The concept of the hot spot is important to understand the anomalous transport phenomena in high- $T_c$  cuprates [24]. When the AF fluctuations with  $\mathbf{Q} = (Q, 0), (0, Q)$  are strong enough, a  $d_{xy}$ -type superconductivity as shown in fig.1 (d) will be realized when  $Q \lesssim 2k_F$ . As shown in fig. 1, the position of the nodes for the s-wave state do not coincide with that of the  $d_{xy}$ -wave state, except for the case of  $Q = 2k_F$ .

In the present paper, we will confirm that (i) a highly anisotropic s-wave SC gap observed in (Y,Lu)Ni<sub>2</sub>B<sub>2</sub>C (e.g.,  $\Delta_{\text{max}}/\Delta_{\text{min}} > 10$ ) can be realized with typical model parameters, and (ii) a relatively higher s-wave  $T_c$  (e.g.,  $T_c \gtrsim T_c^0/2$ ) can be realized under the condition that s-wave  $T_c$  is larger than the d-wave one. In the following sections, we solve the Eliashberg equation and derive the SC order parameter. The obtained region of the model parameters where (i) and (ii) are satisfied is wide enough and consistent with experimental situation in (Y,Lu)Ni<sub>2</sub>B<sub>2</sub>C. Hereafter, we study only the case of  $|\mathbf{Q}| = 2k_F$ , which corresponds to Fig.1 (b).

## III. STRONG COUPLING ELIASHBERG EQUATION

In the preset section, we solve the Eliashberg equation for a singlet paring, and obtain the SC gap function and  $T_c$  for several sets of model parameters. Because the coupling constant  $\lambda \equiv gN(0)$  is of order  $O(1)$  according to experiments, which corresponds to the strong coupling superconductor, we have to work on the strong coupling Eliashberg equation by taking the energy dependence of the gap function,  $\Delta_{\mathbf{k}}(\omega)$ , into account.

The strong coupling Eliashberg equation for the present model within the one-loop approximation at zero temperature is given by [25,26]

$$\Delta_{\mathbf{k}}(\omega) = \frac{1}{Z_{\mathbf{k}}} N(0) \int_{\text{FS}} \frac{d\Omega_{\mathbf{p}}}{2\pi} \int_{\Delta_{\mathbf{p}}^0}^{\infty} dz \text{Re} \frac{\Delta_{\mathbf{p}}(z)}{\sqrt{z^2 - \Delta_{\mathbf{p}}^2(z)}} \cdot \lambda_{\mathbf{k}-\mathbf{p}}(\omega, z) \quad (6)$$

$$\lambda_{\mathbf{k}-\mathbf{p}}(\omega, z) = \int_0^{\infty} dx \frac{1}{\pi} \text{Im} (V^{\text{ph}}(x) - V_{\mathbf{k}-\mathbf{p}}^{\text{AF}}(x))$$

$$\times \left( \frac{1}{\omega + z + x - i\delta} - \frac{1}{\omega - z - x + i\delta} \right) \quad (7)$$

for s-wave SC state, where  $\Delta_{\mathbf{k}}^0$  gives the energy gap, which satisfies that  $\Delta_{\mathbf{k}}^0 = \Delta_{\mathbf{k}}(\Delta_{\mathbf{k}}^0)$ . To simplify the discussion, we neglect the pair breaking effect by the Coulomb interaction  $U$ , that is,  $\mu^* \equiv N(0)U/(1 + N(0)U\ln(W_{\text{band}}/\omega_{\text{ph}})) = 0$  is assumed [25,26]. ( $\mu^*$  is often referred as the Morel-Anderson pseudo-potential.) We also drop the impurity effect, that is, the clean limit case is studied.

In solving the Eliashberg equation at  $T = 0$ , we will not use  $V^{\text{ph}}(\omega)$  given in eq.(2) because it gives an artificial singularity of  $\Delta_{\mathbf{k}}(\omega)$  at  $\omega = \omega_{\text{ph}}$  although it does not influence  $T_c$  as well as  $\Delta_{\mathbf{k}}^0$  badly. To escape the singularity, we use

$$\text{Im}V^{\text{ph}}(\omega + i\delta) = \frac{g\omega_{\text{ph}}}{2} \frac{\Gamma}{(\omega - \omega_{\text{ph}})^2 + \Gamma^2}, \quad (8)$$

where  $\Gamma$  is a positive parameter which is much smaller than  $\omega_{\text{ph}}$ . Equation (8) becomes  $g\omega_{\text{ph}}(\pi/2)\delta(\omega - \omega_{\text{ph}})$  if  $\Gamma$  is infinitesimally small, which is equivalent to eq.(2). Hereafter, we put  $\Gamma = \omega_{\text{ph}}/12$ .

In eqs.(6) and (7),  $V_{\mathbf{k}-\mathbf{p}}^{\text{AF}}(x)$  is given in eq.(3) or eq.(4). Hereafter, we put  $|\mathbf{Q}| = 2k_F$ , which corresponds to Fig.1 (b).  $Z_{\mathbf{k}}$  is the mass enhancement factor at  $\omega = 0$ , which is given by  $Z_{\mathbf{k}} \equiv 1 - \partial\Sigma_{\mathbf{k}}(\omega)/\partial\omega|_{\omega=0}$ , where  $\Sigma_{\mathbf{k}}(\omega)$  is the normal self-energy due to  $V^{\text{ph}}(\omega)$  and  $V_{\mathbf{k}-\mathbf{p}}^{\text{AF}}(\omega)$ . It is expressed at  $T = 0$  as

$$Z_{\mathbf{k}} = 1 + gN(0) + N(0) \int_{\text{FS}} \frac{d\Omega_{\mathbf{p}}}{2\pi} V_{\mathbf{k}-\mathbf{p}}^{\text{AF}}(0). \quad (9)$$

Hereafter, we numerically solve the set of Eliashberg equations, eqs.(6), (7) and (9), under the condition that the gap function has the (anisotropic) s-wave type symmetry, i.e.,  $\Delta_{\mathbf{k}}(\omega)$  has the four-fold rotational symmetry.

In deriving eqs.(6)-(9), we performed the integration with respect to  $\epsilon_{\mathbf{k}}$  first by neglecting the imaginary part of the normal self-energy, which represents the quasiparticle damping rate. The validity of this approximation is apparently violated in high- $T_c$  superconductors because the large  $\text{Im}\Sigma_{\mathbf{k}}(0)(\gg T)$  around the hot spots reduces  $N(0)$ . This effect decreases  $T_c$  much. The validity of this approximation for the present model will be discussed later.

To obtain  $T_c$  both for s-wave and for d-wave, we solve the following Eliashberg equation at finite temperatures [26]:

$$\Delta_{\mathbf{k}}(\omega_n) = -T \sum_m \frac{\pi N(0)}{Z_{\mathbf{k}}} \int_{\text{FS}} \frac{d\Omega_{\mathbf{p}}}{2\pi} \frac{\Delta_{\mathbf{p}}(\omega_m)}{\sqrt{\omega_m^2 + \Delta_{\mathbf{p}}^2(\omega_m)}} \times (V^{\text{ph}}(\omega_n - \omega_m) + V_{\mathbf{k}-\mathbf{p}}^{\text{AF}}(\omega_n - \omega_m)), \quad (10)$$

$$V^{\text{ph}}(\omega_n) = -g \frac{\omega_{\text{ph}}^2}{\omega_n^2 + \omega_{\text{ph}}^2}, \quad (11)$$

$$V_{\mathbf{q}}^{\text{AF}}(\omega_n) = \frac{a \cdot 2^{\alpha-1}}{[1 + \xi_{\text{AF}}^2 |\mathbf{Q} - \mathbf{q}|^2]^{\alpha} + |\omega_n|/\omega_{\text{sf}}}, \quad (12)$$

where  $\omega_n = \pi T(2n + 1)$ , and  $\alpha = 1(2)$  for model 1(2).  $T_c$  is given by the highest temperature for the non-trivial solution of  $\Delta_{\mathbf{k}}(\omega_n)$ , under the constraint that  $\Delta_{k_x, k_y} = c \cdot \Delta_{-k_x, k_y} = c \cdot \Delta_{k_x, -k_y} = \Delta_{-k_x, -k_y}$ , where  $c = 1$  for the (extended) s-wave and  $c = -1$  for the  $d_{xy}$ -wave, respectively. In deriving eq.(10), we used eq.(2), not eq.(8).

## IV. NUMERICAL SOLUTIONS

### A. comparison between model 1 and model 2

Hereafter, we put the phonon parameters as  $\lambda \equiv gN(0) = 1.5$  and  $\omega_{\text{ph}} = 1.0$ ; the latter corresponds to  $\sim 300\text{K}$  experimentally. We stress that the main aim of this work is to present the new mechanism of the point-node like SC gap, not to reproduce the precise experimental value of  $T_c$  and thermodynamic measurements in  $(\text{Y},\text{Lu})\text{Ni}_2\text{B}_2\text{C}$ . Figure 3 shows  $\Delta_{\text{max}}^0 \equiv \Delta_{\theta_k=\pi/4}^0$ ,  $\Delta_{\text{min}}^0 \equiv \Delta_{\theta_k=0}^0$ ,  $T_c$  for s-wave symmetry ( $s$ - $T_c$ ) and  $T_c$  for d-wave one ( $d$ - $T_c$ ) obtained in model 1 for  $\xi_{\text{AF}}^2 = 400$  and  $aN(0) = 0 \sim 600$ . We see that s-wave SC state is realized when  $aN(0) < 380$ . The condition  $\Delta_{\text{max}}^0/\Delta_{\text{min}}^0 > 10$  is realized when  $300 < aN(0) < 380$ , although the realized  $T_c$  is less than one fifth of  $T_c^0 = 0.157$ , which is the transition temperature without AF fluctuations (i.e.,  $aN(0) = 0$ ).

Next, we study the model 2: Figure 4 shows  $\Delta_{\text{max}}^0$ ,  $\Delta_{\text{min}}^0$ ,  $s$ - $T_c$  and  $d$ - $T_c$  for  $\omega_{\text{sf}} = 0.1$  in model 2. We see that the condition  $\Delta_{\text{max}}^0/\Delta_{\text{min}}^0 > 10$  is realized for much wider range of  $aN(0)$  for  $\xi_{\text{AF}}^2 = 50 \sim 200$ . In addition, the realized s-wave  $T_c$  is higher than the half of  $T_c^0$ .

As a result, in both model 1 and model 2, a highly anisotropic SC gap is realized under the condition of  $s$ - $T_c > d$ - $T_c$ . However, the obtained s-wave  $T_c$  is much higher in model 2, and the condition for a strong anisotropy (say  $\Delta_{\text{max}}/\Delta_{\text{min}} > 10$ ) is much easier. The reason is that the slow tail of model 1 for  $\mathbf{q}$  away from  $\mathbf{Q}$ , which follows the lorenzian form, does not contribute to make SC gap minima, but work as a pair breaking effect like the momentum independent Coulomb interaction does. (see Fig. 2.)

We note that the lorenzian type slow tail of model 1 might not be natural because the peak of  $\chi_{\mathbf{q}}(\omega)$ , which is created by the nesting of the FS, will decays faster once the nesting condition becomes ill as  $\mathbf{q}$  is away from  $\mathbf{Q}$ . In reality,  $\chi_{\mathbf{q}}(0)$  for high- $T_c$  cuprates obtained by the FLEX approximation, which is shown in Fig. 11 of ref. [24] for example, seems to decay faster than the lorenzian form. In that figure, we also see that  $\chi_{\mathbf{q}}(\omega)$  takes an almost constant value ( $\sim 0.5U^{-1}$ ) when  $|\mathbf{q} - \mathbf{Q}| \gg \xi_{\text{AF}}^{-1}$ , so it will work as a pair breaking effect. As a result, the total Morel-Anderson pseudo-potential will be  $\mu_{\text{AF}}^* + \mu^* \sim 2\mu^*$ ,

where  $\mu^* \equiv N(0)U/(1 + N(0)U\ln(W_{\text{band}}/\omega_{\text{ph}}))$ . Hereafter, we study the condition of realizing the deep SC gap minima and analyze its property based on the model 2 in more detail, by putting  $\mu^* = 0$ . The reader have to remind that the obtained  $T_c$  in later sections is overestimated in that the pair breaking effect is neglected.

## B. gap functions in model 2

Figure 5 shows  $\Delta_{\max}$ ,  $\Delta_{\min}$ , s- $T_c$  and d- $T_c$  obtained in model 2 for  $\xi_{\text{AF}}^2 = 200$ . The  $\omega_{\text{sf}}$ -dependence of  $\Delta_{\max,\min}$  and s- $T_c$  is very weak, while that of d- $T_c$  is strong. For  $\omega_{\text{sf}} = 0.1$ ,  $\Delta_{\max}/\Delta_{\min} > 10$  is realized for  $aN(0) > 280$ , and the condition s- $T_c > d-T_c = 0.075$  is satisfied when  $aN(0) < 490$ .

Here, we discuss about the adequacy of parameters used in the present calculation. The relatively large value of  $\xi_{\text{AF}}$  used in the present analysis is consistent with the prominent AF fluctuations in (Y,Lu)Ni<sub>2</sub>B<sub>2</sub>C at lower temperatures [7,8]. Then, the smaller value of  $\omega_{\text{sf}}$  is also expected because  $\omega_{\text{sf}} \propto \xi_{\text{AF}}^{-2}$ . Note that  $\omega_{\text{sf}} \sim T$  and  $\xi_{\text{AF}}^2 \propto T^2$  are realized in an optimum high- $T_c$  cuprates, which is reproduced by the FLEX approximation [24]. Moreover, the coupling constant for AF fluctuations,  $aN(0)$ , which corresponds to  $N(0)(3U^2/2)\chi_{\mathbf{Q}}(0)$  within the RPA or FLEX approximation, will be smaller than that of high- $T_c$  cuprates because  $U/W_{\text{band}}$  in (Y,Lu)Ni<sub>2</sub>B<sub>2</sub>C is smaller. As one can see in Fig. 5, similar strongly anisotropic gaps are obtained for wider range of parameters when  $\xi_{\text{AF}}^2 = 50 \sim 400$ .

Figure 6 shows the  $\mathbf{k}$ -dependence of  $\Delta_{\mathbf{k}}^0$  on the Fermi surface, for  $aN(0) = 0 \sim 400$ . (Note that  $\theta_{\mathbf{k}} = \tan^{-1}(k_x/k_y)$ .) Thus, the s-wave SC gap with deep point minima is realized for  $aN(0) > 300$ . It is similar to (s+g)-wave SC gap function proposed in ref. [27], where the impurity effect on the shape of  $\Delta_{\mathbf{k}}^0$  is analyzed. We stress that a model with almost the same strength of attractive interactions both for the s-wave and for the g-wave channels, which was just introduced as an assumption in ref. [27], is derived microscopically in the present study.

Figure 7 shows the  $\epsilon$ -dependence of  $\Delta_{\mathbf{k}}(\epsilon)$ . Note that  $\Delta_{\mathbf{k}}(\Delta_{\mathbf{k}}^0) = \Delta_{\mathbf{k}}^0$  gives the energy-gap of the SC order parameter. We comment that  $\Gamma = \omega_{\text{ph}}/6$  in eq.(8) is assumed only in deriving Fig. 7, although  $\Gamma = \omega_{\text{ph}}/12$  is used in other figures. (By this reason,  $\Delta_{\mathbf{k}}^0$  for  $aN(0) = 0$  is smaller than 0.3 only in Fig. 7.) In Fig. 7, we note that  $\Delta_{\min}(\epsilon)$  (for  $\theta_{\mathbf{k}} = 0$ ) increases as  $\epsilon$  increases from  $\Delta_{\min}^0$ . Such an energy dependence of  $\Delta_{\min}(\epsilon)$  will stabilize the solution for the strongly anisotropic s-wave SC state in eq.(6). This effect, which is dropped within the weak coupling BCS theory, means the importance of the strong coupling effect for realizing the strongly anisotropic SC gap.

At finite temperatures, the gap function  $\Delta_{\mathbf{k}}(\epsilon_n)$  is obtained by solving the strong coupling Eliashberg equa-

tion for Matsubara frequencies, eq (10). Then, the gap function for real  $\epsilon$ ,  $\Delta_{\mathbf{k}}(\epsilon)$ , is given by the numerical analytic continuation with high accuracy. Here, we study several physical quantities at finite temperatures using the obtained  $\Delta_{\mathbf{k}}(\epsilon)$ : Figure 8 show the derived DOS for  $\xi_{\text{AF}}^2 = 200$  and  $aN(0) = 0 \sim 400$ , which is given by

$$\begin{aligned} \rho(\epsilon) &= \sum_{\mathbf{k}} \text{Im}G_{\mathbf{k}}(\omega - \delta)/\pi \\ &= N(0) \int_{\text{FS}} \frac{d\Omega_{\mathbf{k}}}{2\pi} \text{Re} \frac{|\epsilon|}{\sqrt{\epsilon^2 - \Delta_{\mathbf{k}}^2(\epsilon)}}. \end{aligned} \quad (13)$$

We put  $N(0) = 1$  in Fig. 8. It is shown that the finite DOS at lower energies emerges as the coupling constant for AF fluctuations,  $aN(0)$ , increases. We can also calculate the nuclear-lattice relaxation ratio ( $T_1$ ) and the ultrasonic attenuation ratio ( $\alpha$ ). Figure 9 shows the obtained  $1/T_1T$  and  $\alpha$ , which are given by

$$\begin{aligned} R_{\pm} &= N(0) \int_{\text{FS}} \frac{d\Omega_{\mathbf{k}}}{2\pi} \int_0^{\infty} dz \left( -\frac{df}{dz} \right) \\ &\quad \times 2 ([g_{\mathbf{k}}(z)]^2 \pm [f_{\mathbf{k}}(z)]^2), \end{aligned} \quad (14)$$

$$g_{\mathbf{k}}(z) \equiv \int d\epsilon_{\mathbf{k}} \text{Im}G_{\mathbf{k}}(z - i\delta)/\pi = \text{Re} \frac{z}{\sqrt{z^2 - \Delta_{\mathbf{k}}^2(z)}}, \quad (15)$$

$$f_{\mathbf{k}}(z) \equiv \int d\epsilon_{\mathbf{k}} \text{Im}F_{\mathbf{k}}(z - i\delta)/\pi = \text{Re} \frac{\Delta_{\mathbf{k}}(z)}{\sqrt{z^2 - \Delta_{\mathbf{k}}^2(z)}}, \quad (16)$$

where  $1/T_1T = R_+$  and  $\alpha = R_-$ , respectively. We note that  $\alpha$  in eq. (16) is derived by taking the average of the momentum of the absorbed phonon, which might be different from the experimental situation. In Fig. 9,  $1/T_1T$  for  $aN(0) = 0$  shows a large coherence peak below  $T_c$ . However, it is smaller than that given by the weak coupling BCS theory in the present model because the peak of the DOS is smeared out due to the strong coupling effect, that is, finite  $\text{Im}\Delta_{\mathbf{k}}(\epsilon)$  at finite temperatures. The coherence peak is further suppressed as  $aN(0)$  increases.

We comment that the coherence peak is further suppressed or vanishes if we take account of the effect of the finite quasiparticle damping rate,  $\gamma_{\mathbf{k}} = \text{Im}\Sigma_{\mathbf{k}}(-i\delta)$ , at finite temperatures, because finite  $\gamma_{\mathbf{k}}$  reduce the DOS at  $\epsilon = 0$ . However, this effect cannot be included in eq.(10) because the following relation:

$$\int_{-\infty}^{\infty} d\epsilon_{\mathbf{k}} \hat{G}_{\mathbf{k}}(\omega_n) = -\pi \frac{i\omega_n Z_{\mathbf{k}} \hat{1} + \Delta_{\mathbf{k}}(\omega_n) \hat{\sigma}_x}{\sqrt{[\omega_n Z_{\mathbf{k}}]^2 + \Delta_{\mathbf{k}}^2(\omega_n)}}, \quad (17)$$

which is given by dropping the self-energy except for its  $\omega_n$ -linear term,  $(-Z_{\mathbf{k}} + 1)i\omega_n$ , has been used in deriving eq.(10). In eq.(17),  $\hat{G}_{\mathbf{k}}(\omega_n)$  is the  $2 \times 2$  Green function in Nambu representation, and  $\hat{\sigma}_x$  is the Pauli matrix. To take the effect of  $\gamma_{\mathbf{k}}$  into account, which has been very important in the case of high- $T_c$  superconductors, we have to perform the  $\epsilon_{\mathbf{k}}$ -integration “numerically” instead of using eq.(17). We further comment that the anisotropy of the dispersion for conduction electrons, which is totally

neglected in the present model, will decrease the coherence peak because a small  $\mathbf{k}$ -dependence of  $\Delta_{\mathbf{k}}$  emerges even in the absence of the AF fluctuations. By these two reasons mentioned above, the tiny coherence peak for  $aN(0) > 300$  may vanish after all. Note that a tiny coherence peak exists even in the case of  $d$ -wave within the BCS theory if the momentum dependence of  $N(0)$  is totally neglected.

Figure 9 also shows the  $\log(1/T_1 T) - \log T$  plot for  $aN(0) = 0 \sim 400$ . This plot shows that the temperature dependence of  $1/T_1$  at lower temperatures changes from an exponential behavior to a  $T^3$ -behavior for  $aN(0) > 200$ , reflecting the finite DOS at lower energies around the hot spots. In a three-dimensional (3D) model, the relation  $1/T_1 \propto T^3$  corresponds to the line-node SC gap. If a point-node SC gap occurs in a 3D system owing to the present mechanism,  $1/T_1 \propto T^5$  will be observed.

Before closing this section, we comment that the mass enhancement factor  $Z_{\mathbf{k}}$  is the function of the energy in the original Eliashberg equation. In the present work, however, we dropped the energy dependence for the simplicity of the analysis. It will be allowed for the purpose of the present study, although it is not for calculating the fine structure of the superconducting DOS. In Fig. 10, we show the solution of the Eliashberg equation given by eqs. (6) and (9) as well as the solution given by taking the energy-dependence of  $Z_{\mathbf{k}}(\omega)$  into account correctly. We see that the ratio of the gap anisotropy,  $\Delta_{\max}^0/\Delta_{\min}^0$ , is enlarged a bit, by performing a more accurate calculation. In more detail,  $\Delta_{\max}^0$  is enlarged about 20% whereas  $\Delta_{\min}^0$  (at the hot spot) increases only slightly, because the influence of the SC gap function on  $Z_{\mathbf{k}}$  is little at the hot spot. We have also checked that the influence of the energy-dependence of  $Z_{\mathbf{k}}$  on  $T_c$  is small.

## V. COMPARISON WITH THE WEAK COUPLING BCS THEORY

In the previous section, we have shown that the s-wave superconductivity with deep gap minima is reproduced easily by solving the strong-coupling Eliashberg equation for  $\lambda \equiv gN(0) = 1.5$ . That is, a large anisotropic ratio  $\Delta_{\max}/\Delta_{\min} > 10$  is realized under the condition of  $s\text{-}T_c > d\text{-}T_c$ , by assuming reasonable model parameters. In this section, we study the same model within the weak-coupling BCS theory for a smaller value of  $\lambda$ , and show that the strong-coupling analysis performed in previous sections is indispensable for reproducing the strongly anisotropic s-wave SC state.

In the weak coupling BCS theory, energy dependence of the gap function as well as the normal self-energy are dropped. Thus, the corresponding Eliashberg equation is given in eq.(6) (or eq.(10)) by (i) putting  $\omega = 0$  ( $\omega_n = 0$ ), (ii) replacing  $\Delta_{\mathbf{k}}(\epsilon)$  ( $\Delta_{\mathbf{k}}(\epsilon_n)$ ) with  $\Delta_{\mathbf{k}}^0$ , and (iii) putting  $Z_{\mathbf{k}} = 1$ . The obtained  $\Delta_{\min,\max}$  and  $s\text{-}d\text{-}T_c$  is shown in Fig.11, which are denoted as “BCS”. Here, we put

$\lambda = gN(0) = 0.7$  to justify the weak coupling treatment. We see that the  $s\text{-}T_c > d_{xy}\text{-}T_c$  is realized only for  $aN(0) < 50$ , where the anisotropy of the s-wave SC gap is very weak. Thus, the strong anisotropic s-wave SC gap cannot be obtained by the BCS theory.

Such a high  $d_{xy}\text{-}T_c$  given by the “BCS” theory is suppressed drastically in the strong-coupling analysis, mainly due to the mass-enhancement factor;  $Z_{\mathbf{k}} > 1$ . To show this fact, we also study the weak coupling BCS theory, by taking the “renormalization” by  $Z_{\mathbf{k}}$  into account correctly. We call it the “R-BCS” theory, where the Eliashberg equation is given in eq.(6) (or eq.(10)) by performing the simplification (i) and (ii) only. The obtained  $\mathbf{k}$ -dependence of  $Z_{\mathbf{k}}$  is shown in Fig.12. We see that  $Z_{\mathbf{k}}$  takes large values around the hot spots, so it will mainly reduce the effect of the AF fluctuations in the Eliashberg equation. The obtained result for  $gN(0) = 1.0$  by the R-BCS theory is shown in Fig. 11. We see that  $d_{xy}\text{-}T_c$  is strongly reduced by the factor  $Z_{\mathbf{k}}$ , so  $s\text{-}T_c > d_{xy}\text{-}T_c$  is realized till much larger value of  $aN(0)$ ;  $aN(0) < 240$ . Thus,  $\Delta_{\max}/\Delta_{\min} \lesssim 5$  can be realized within the R-BCS theory.

As a result, the renormalization effect by  $Z_{\mathbf{k}}$  is important to realize the highly anisotropic s-wave SC gap. However, R-BCS theory is still insufficient for a quantitative study, so one have to work on the strong coupling Eliashberg equation, eq. (6) or eq. (10), for  $gN(0) \sim O(1)$ .

Finally, we comment that the DOS around the hot spots will decrease appreciably owing to the finite  $\gamma_{\mathbf{k}}$  because  $\gamma_{\mathbf{k}}$  takes a large value at the hot spots when the AF fluctuations are strong, as  $Z_{\mathbf{k}}$  does. This effect was found to reduce the  $T_c$  prominently in the case of high- $T_c$  superconductors. To take this effect into account, we have to perform the  $\epsilon_{\mathbf{k}}$ -integration “numerically” instead of using eq.(17). In this respect, the obtained  $d_{xy}\text{-}T_c$  in the present work may be over-estimated.

## VI. DISCUSSIONS

### A. condition for the strongly anisotropic s-wave SC gap in 3D systems

In the present paper, we proposed a mechanism of the s-wave superconductivity with deep gap minima in the presence of AF fluctuations. We found that a highly anisotropic SC gap observed in (Y,Lu)Ni<sub>2</sub>B<sub>2</sub>C can be reproduced with reasonable model parameters. Here, we summarize the obtained condition for realizing the deep SC gap minima:

(i) To make  $\Delta_{\max}^0/\Delta_{\min}^0 \gg 1$ ; a strong e-p coupling (e.g.,  $\lambda \equiv gN(0) > 1$ ) as well as larger  $\xi_{\text{AF}}^2$  (e.g.,  $\xi_{\text{AF}}^2 > 50$ ) is required. The “radius of the minima” in the SC gap will be  $\sim \xi_{\text{AF}}^{-1}$ . The strong coupling Eliashberg equation should be solved for a reliable analysis.

(ii) To make  $s-T_c > d-T_c$ ; in addition to a strong e-p coupling, a smaller coupling constant between electrons and AF fluctuations (e.g.,  $aN(0)/\xi_{AF}^2 < 1$ ) as well as a small energy scale of AF fluctuations (e.g.,  $\omega_{sf} \ll \omega_{ph}$ ) is required. In addition, the nesting area of the FS should be small. This condition will be easily satisfied in a three-dimensional system with several FS's. This fact will be discussed later in more detail.

Here, the shape of the FS is chosen to be circle. The most essential effect of the anisotropy as well as the dimensionality of the FS will appear in  $d-T_c$ , because it is enhanced when the nesting of the FS which is consistent with the main AF fluctuations exists, while  $s-T_c$  and s-wave gap function will be rather insensitive. Thus, the  $d-T_c$  obtained here may have only a qualitative meaning. Nonetheless, the realized  $d-T_c$  will remain small if one analyze a three dimensional (3D) system. In fact, refs. [28–31] discuss that the  $d-T_c$  due to AF fluctuations in 3D systems remains low because the nesting area in 3D FS is small in general. In addition, the region of parameters for  $d-T_c$  is also very restricted in 3D systems. According to a band calculation for  $YNi_2B_2C$ , the shape of the FS is 3D like, and the nesting area of the FS is only 4.3%, which is supported experimentally by a tiny change of the resistivity at  $T = T_N$  [13].

As a result,  $d-T_c$  will not be high in the real three dimensional FS for  $(Y, Lu)Ni_2B_2C$ , so the mechanism of s-wave SC gap with deep minima proposed in the present paper will be realized in  $(Y, Lu)Ni_2B_2C$  without difficulty. In general, the weight of the nesting area in the FS decreases further if several FS's exists like in heavy fermion systems. Although the present study is based on a simplified two dimensional model, the mechanism of the anisotropic s-wave SC gap due to AF fluctuations proposed in the present work will be universal. We also note that the effect the finite  $\gamma_{\mathbf{k}} = \text{Im}\Sigma_{\mathbf{k}}(-i\delta)$  at  $T = T_c$ , which will reduce  $d-T_c$  as mentioned in the previous section, is not taken into account in the present analysis. In this sense, the obtained  $d-T_c$  is overestimated.

Finally, we shortly discuss the location of the gap minima in 3D systems. Figure 13 shows the expected location of the gap minima for (a)  $|\mathbf{Q}| = 2k_F$  and (b)  $|\mathbf{Q}| < 2k_F$  ( $\mathbf{Q} \parallel \hat{x}$  in both cases) in the case of the spherical FS whose radius is  $k_F$ . In case (a), point minima occur at two points on the  $x$ -axis. In case (b), on the other hand, gap minima will make two small circles. Therefore, gap minima will be short lines or small circles in real 3D systems with anisotropic FS's. Obviously, the depth of the gap minima should depend on the position: The deepest point will be on the portion of the FS where  $\lambda$  or the density of states at  $\mathbf{k}$ ,  $\text{Im}G_{\mathbf{k}}(-i\delta)/\pi$ , takes relatively a smaller value. In such a case, the deepest point of the gap may cause “point-node like behaviors” in various thermodynamical quantities at lower temperatures, even in case (b) ( $|\mathbf{Q}| < 2k_F$ ).

For a more detailed study, a strong coupling study based on a microscopic Hamiltonian with 3D FS's is highly demanded. For example, an analysis of a Holstein-

Hubbard model by the FLEX approximation will be fruitful.

## B. possibility of the $(s+id)$ -wave superconductivity: breakdown of the time reversal symmetry

In figs. 4 and 5, we obtained  $s-T_c$  and  $d-T_c$  by considering the transition from the normal state. In the case of  $s-T_c \gg d-T_c$  ( $d-T_c \gg s-T_c$ ), a pure  $s(d)$ -wave SC state will be realized whole the temperature region below  $s(d)-T_c$  because the established  $s(d)$ -wave SC gap will prevent the emergence of the  $d(s)$ -wave gap. However, it is an interesting question whether s-wave SC gap and d-wave one coexist or not when  $d-T_c \sim s-T_c$  below  $\min\{d-T_c, s-T_c\}$ . In this case, the gap function will be given by  $\Delta_{\mathbf{k}}^0 = \Delta_{\mathbf{k}}^{s0} + e^{i\phi}\Delta_{\mathbf{k}}^{d0}$ , where we choose the  $U(1)$  gauge to make both  $\Delta_{\mathbf{k}}^{s0} (\propto 1)$  and  $\Delta_{\mathbf{k}}^{d0} (\propto k_x k_y)$  real. Then,  $e^{i\phi} = i$  is required to make the gain of the condensation energy largest, at least within the weak-coupling theory, because  $\langle \Delta_{\mathbf{k}}^0 \rangle_{\text{FS}}$  takes the maximum value then. The  $(s+id)$ -wave superconductivity is a very interesting state in that the time reversal symmetry (TRS) is broken. In a later publication, we will study the nature of the superconducting state whole the temperature region in more detail [32].

Here, we notice that some of the deep minima on a s-wave SC gap caused by the mechanism proposed in the present work might be filled to some extent once the system changes from the s-wave SC state to the  $(s+id)$ -wave state as the temperature decreases. In the present model, in fact, the position of the “point minima” in the anisotropic s-wave state is different from that of the  $d_{x^2-y^2}$ -wave state except for the case of  $|\mathbf{Q}| = 2k_F$ , as shown in Fig. 1. We expect that a pure s-wave state is realized in  $(Y, Lu)Ni_2B_2C$  because the nesting area of the FS is very small, which suggestss that  $s-T_c \ll d-T_c$  as discussed before.

## C. consideration on other materials: $\text{Sr}_2\text{RuO}_4$ , $\text{PrOs}_4\text{Sb}_{12}$ , $\text{Na}_{0.33}\text{CoO}_2$

First, we stress that the proposed mechanism here can make deep SC gap minima also in a unconventional (p-wave or d-wave) superconductors besides the original nodes: When a unconventional superconductivity is realized by a Kohn-Luttinger type mechanism, which is free from the concept of the QCP, some magnetic fluctuations owing to the nesting of the FS will make “deep gap minima” on the SC gap function, if their energy scale is too low to produce a different type unconventional superconductivity. Many heavy fermions and transition metal oxides superconductors have been reproduced properly in terms of the Kohn-Luttinger type mechanism, using the perturbation theory with respect to  $U$  [33]. In Appendix,

we study a model which shows the p-wave superconductivity with full gap, and find that the deep gap minima emerges on the SC gap function as the AF fluctuations increases.

In a similar context, we would like to explain the theoretical study for  $\text{Sr}_2\text{RuO}_4$  by Nomura and Yamada [34]:  $\text{Sr}_2\text{RuO}_4$  shows a spin-triplet SC state at  $T_c = 1.5\text{K}$ . Based on the third-order and forth-order perturbation theory, they found that the p-wave superconductivity occurs in  $\text{Sr}_2\text{RuO}_4$ . According to their analysis, a large and isotropic (chiral p-wave) SC gap opens on the  $\gamma$ -FS, whereas small and strongly anisotropic gaps occur on  $\alpha, \beta$ -FS's. The obtained SC gap function is consistent with the specific heat measurement below  $T_c$ . It is also consistent with the recent heat conductivity measurement under the rotatable magnetic field [35]. We note that the almost gap-less SC gap realized in  $\text{Sr}_2\text{RuO}_4$  originates from the cancellation of the pairing interaction.

$\text{PrOs}_4\text{Sb}_{12}$  is a Pr-filled Skutterudite superconducting compound, with  $T_c = 1.85\text{K}$  [36,37]. In  $\text{PrOs}_4\text{Sb}_{12}$ , considerable magnetic (dynamical) fluctuations are observed by  $\mu$ -SR measurement [38] and by neutron diffraction measurement below  $4\text{K}$  [39]. Moreover, e-p coupling will be also strong in  $\text{PrOs}_4\text{Sb}_{12}$  because various Pr-filled Skutterudite compounds are conventional s-wave superconductors with relatively high  $T_c$ 's.

The symmetry of the SC gap is not determined now. According to the heat conductivity measurement under the rotatable magnetic field, the SC gap has four point nodes along [100] and [010] axes in a higher magnetic-field phase, whereas two point nodes along [010] axis disappear in a lower magnetic-field phase [41]. One may expect that the strongly anisotropic s-wave SC state is realized in  $\text{PrOs}_4\text{Sb}_{12}$ , considering that the small energy scale of the AF fluctuations observed by neutron diffraction ( $\omega_{\text{sf}} \sim 0.5\text{meV}$ ) [39] is appropriate for making the deep SC gap minima as shown in the present paper. Moreover, a recent  $\mu$ -SR measurement suggests that the TRS is broken in the SC state of  $\text{PrOs}_4\text{Sb}_{12}$  [38]. It may be a (s+id)-wave SC state [40], which could be reproduced by the mechanism proposed in the present work as discussed in the previous subsection.

$\text{Na}_{0.33}\text{CoO}_2$  is a triangular lattice cobalt oxide superconductor, with  $T_c = 4.5\text{K}$ . The symmetry of the SC gap is also under debate now. According to NMR/NQR measurements,  $1/T_1T$  in a sample with magnetic fluctuations shows no coherence peak, and  $1/T_1 \propto T^3$  is observed below  $T_c$  [42,43]. On the other hand,  $1/T_1T$  in a sample with less magnetic fluctuations shows a tiny coherence peak [44]. The reduction ratio of  $T_c$  due to impurities,  $-dT_c/dx$  ( $x$  being the concentration of impurities), seems to be too small as a unconventional superconductor. These measurements might be able to be explained as a s-wave superconductor with deep gap minima caused by the mechanism proposed in the present paper, as is the case with  $(\text{Y},\text{Lu})\text{Ni}_2\text{B}_2\text{C}$ .

In both  $\text{PrOs}_4\text{Sb}_{12}$  and  $\text{Na}_{0.33}\text{CoO}_2$ , more experimen-

tal and theoretical studies are required to determine the symmetry and the mechanism of the superconductivity. In future, the present study will offer a hint to understand various SC compounds in the presence of both e-p couplings and magnetic fluctuations.

#### D. summary

In summary, we studied the influence of the AF fluctuations on the SC gap function  $\Delta_{\mathbf{k}}(\epsilon)$  with s-wave symmetry owing to the strong e-p coupling, by analyzing the strong coupling Eliashberg equation. We confirmed that deep SC gap minima emerge in  $\Delta_{\mathbf{k}}(\epsilon)$  as the AF fluctuation increases. The condition for the realization of strong anisotropy (say  $\Delta_{\text{max}}^0/\Delta_{\text{min}}^0 > 10$ ) is studied in detail. We stress again that the main aim of this work is to present the new mechanism of the point-node like SC gap, not to reproduce the precise value of  $T_c$  and thermodynamic measurements in  $(\text{Y},\text{Lu})\text{Ni}_2\text{B}_2\text{C}$ .

According to the present mechanism, (groups of) pair of gap minima appear at points on the Fermi surface which are connected by the nesting vector  $\mathbf{Q}$ , in both cases of s-wave superconductors and non s-wave ones. Their position is equal to the hot spots, where the quasi-particle damping rate  $\gamma_{\mathbf{k}}$  caused by the magnetic fluctuations takes the (local) maximum value. The present mechanism is expected to reproduce the point-node like SC gap in  $(\text{Y},\text{Lu})\text{Ni}_2\text{B}_2\text{C}$ , as well as the direction of the point minima. It is a future problem to determine the precise positions of the gap minima on the FS's by taking account of the realistic shape of FS's.

To realize a higher s- $T_c$  ( $\gg d-T_c$ ), it is desired that the position of the point minima (hot spots) is away from the van-Hove singular point, because  $\lambda$  is expected to take a larger value there. In case there are several hot spots, the deepest point gap minima will appear on the FS where  $\lambda$  takes the smallest value. Deep SC gap minima in the SC gap due to AF fluctuations proposed in the present work are expected to emerge even in unconventional superconductors, as explained in Appendix. In addition, recently found exotic superconductors,  $\text{PrOs}_4\text{Sb}_{12}$  and  $\text{Na}_{0.33}\text{CoO}_2$ , were briefly discussed from the viewpoint of the present study.

The author is grateful to Y. Matsuda, K. Izawa and J.P. Brison for useful discussions about experiments on  $(\text{Y},\text{Lu})\text{Ni}_2\text{B}_2\text{C}$ . He is also grateful to M. Sato, H. Yoshimura and K. Ishida for valuable comments on NMR/NQR. For useful discussions on theory, he is thankful to K. Yamada, T. Sato, H. Kohno, H. Ikeda and T. Nomura.

## APPENDIX A: IN THE CASE OF THE P-WAVE SUPERCONDUCTOR

As discussed in §VI, the deep SC gap minima at the hot spots owing to the AF fluctuations proposed in the present paper will also be realized in the case of p- or d-wave superconductor. To confirm this fact, we study a p-wave superconducting systems with AF fluctuations, and see that the deep SC gap minima emerge as the AF fluctuations increases. In general, the odd-parity SC gap function in the Nambu representation is given by

$$\hat{\Delta}_{\mathbf{k}} = \mathbf{d}_{\mathbf{k}} \cdot i\vec{\sigma}\sigma_y, \quad (\text{A1})$$

where  $\mathbf{d}_{\mathbf{k}}$  is the d-vector. The quasiparticle energy gap is given by  $\sqrt{\mathbf{d}_{\mathbf{k}}^* \cdot \mathbf{d}_{\mathbf{k}}}$ .

Here, we introduce the following paring potential for the p-wave channel in two dimension:

$$V_{\mathbf{k},\mathbf{k}'}^{\text{p-ch}}(\omega_n) = -g \frac{\omega_p^2}{\omega_n^2 + \omega_p^2} \cdot 2 \cos(\theta_{\mathbf{k}} - \theta_{\mathbf{k}}'), \quad (\text{A2})$$

whose diagrammatic expression is shown in Fig. 14. In the presence of the AF fluctuations, the system has the tetragonal symmetry ( $D_{4h}$ ). In this case, six p-wave pairing states with different symmetries give the same quasiparticle gap without nodes, which is expected to optimize the condensation energy at least within the weak coupling theory [45]. In each pairing state,  $\mathbf{d}_{\mathbf{k}}(\omega)$  is composed of  $(\Delta_{\mathbf{k}}^{(1)}(\omega), \Delta_{\mathbf{k}}^{(2)}(\omega))$ , which changes under the point group operations as  $(\hat{k}_x, \hat{k}_y)$ . We promise that both  $\Delta_{\mathbf{k}}^{(1)}(0)$  and  $\Delta_{\mathbf{k}}^{(2)}(0)$  are real. For example, the chiral p-wave state is given by  $\mathbf{d}_{\mathbf{k}}(\omega) \equiv \hat{\mathbf{z}}(\Delta_{\mathbf{k}}^{(1)}(\omega) \pm i\Delta_{\mathbf{k}}^{(2)}(\omega))$ . Then, the strong coupling Eliashberg equation for the p-wave symmetry with full gap is given by

$$\Delta_{\mathbf{k}}^{(j)}(\omega_n) = -T \sum_m \frac{\pi N(0)}{Z_{\mathbf{k}}} \int_{\text{FS}} \frac{d\Omega_{\mathbf{p}}}{2\pi} \frac{\Delta_{\mathbf{p}}^{(j)}(\omega_m)}{\sqrt{\omega_m^2 + D_{\mathbf{p}}^2(\omega_m)}} \times \left( V_{\mathbf{k},\mathbf{p}}^{\text{p-ch}}(\omega_n - \omega_m) + \frac{-1}{3} V_{\mathbf{k}-\mathbf{p}}^{\text{AF}}(\omega_n - \omega_m) \right), \quad (\text{A3})$$

where  $j = 1, 2$ ,  $D_{\mathbf{p}}^2(\omega) \equiv \{\Delta_{\mathbf{p}}^{(1)}(\omega)\}^2 + \{\Delta_{\mathbf{p}}^{(2)}(\omega)\}^2$ , and  $V_{\mathbf{k}-\mathbf{p}}^{\text{AF}}(\omega_n)$  represents the interaction due to AF fluctuations introduced in eq.(12). Note that the factor  $-1/3$  in front of  $V_{\mathbf{k}-\mathbf{p}}^{\text{AF}}$  comes from the fact that  $\langle \vec{s} \cdot \vec{s}' \rangle_{S=1} = (-1/3) \langle \vec{s} \cdot \vec{s}' \rangle_{S=0} = 1/4$ . Because of the relation  $\cos(\theta_{\mathbf{k}} - \theta_{-\mathbf{k}}) = -1$ , the expression for  $Z_{\mathbf{k}}$  in eq.(A3) is same as that in eq.(9).

Here, we study eq.(A3) numerically, by putting  $g = \omega_p = 1.0$ . The quasiparticle gap is given by the relation  $\Delta_{\mathbf{k}}^0 \equiv |D_{\mathbf{k}}(\Delta_{\mathbf{k}}^0)|$ . The upper panel in Fig. 15 shows the obtained  $\Delta_{\text{max}}^0 \equiv \Delta_{\theta_{\mathbf{k}}=0}^0$  and  $\Delta_{\text{min}}^0 \equiv \Delta_{\theta_{\mathbf{k}}=\pi/4}^0$  for the p-wave SC state at zero temperatures, as functions of the AF coupling constant  $aN(0)$ . (Note that  $|\Delta_{\mathbf{k}}|$  is constant when  $aN(0) = 0$ .) The lower panel shows the obtained

$T_c$ 's both for p-wave and d-wave. As shown in Fig. 15, deep minima emerges in the p-wave SC gap owing to the AF fluctuations. Quantitatively speaking, however, the obtained ratio  $\Delta_{\text{max}}/\Delta_{\text{min}}$  in the present model is smaller than that in Fig. 5 at a fixed  $aN(0)$ , because of the factor  $1/3$  in front of  $V_{\text{AF}}$  in eq.(A3).

---

- [1] R.J. Cava, H. Takagi, H.W. Zandbergen, J.J. Krajewski, W.F. Peck Jr, T. Siegrist, B. Batlogg, R.B. van Dover, R.J. Felder, K. Mizuhashi, J.O. Lee, H. Eisaki and S. Uchida : Nature **367** (1994) 252.
- [2] J. Zarestky, C. Stassis, A.I. Goldman, P.C. Canfield, P. Dervenagias, B.K. Cho, and D. C. Johnston: Phys. Rev. **B51** (1995) 678; S.K. Sinha, J.W. Lynn, T.E. Grigereit, Z. Hossain, L.C. Gupta, R. Nagarajan, and C. Godart: Phys. Rev. **B51** (1995) 681.
- [3] A.I. Goldman, C. Stassis, P.C. Canfield, J. Zarestky, P. Dervenagias, B.K. Cho, D.C. Johnston, and B. Sternlieb: Phys. Rev. **B50** (1994) 9668; T. Vogt, A. Goldman, B. Sternlieb, and C. Stassis: Phys. Rev. Lett. **75** (1995) 2628.
- [4] M. Nohara, M. Isshiki, F. Sakai and H. Takagi: J. Phys. Soc. Jpn **68** (1999) 1078.
- [5] K. Izawa, K. Kamata, Y. Nakjima, Y. Matsuda, T. Watanabe, N. Nohara, H. Takagi, P. Thalmeier and K. Maki: Phys. Rev. Lett. **89** (2002) 137006-1.
- [6] Watanabe et al.: Autumn Meeting of Physical Society of Japan (2003).
- [7] T. Kohara, T. Oda, K. Ueda, Y. Yamada, A. Mahajan, K. Elanlumaran, Zakir Hossian, L.C. Gupta, R. Nagarajan, R. Vijayaraghavan and Chandan Mazumdar: Phys. Rev. **B51** (1995) 3985.
- [8] K. Ikushima, J. Kikuchi, H. Yasuka, J. Cava, H. Takagi, J.J. Krajewski and W.W. Peck, Jr.: J. Phys. Soc. Jpn **63** (1994) 2878.
- [9] T. Moriya and K. Ueda: Adv. Physics **49** (2000) 555.
- [10] J.Y. Rhee, X. Wang, and B.N. Harmon: Phys. Rev. B **51** (1995) 15585.
- [11] W.E. Pickett and D.J. Singh: Phys. Rev. Lett. **72** (1994) 3702.
- [12] L.F. Mattheiss: Phys. Rev. B **49** (1994) 13279.
- [13] S.B. Dugdale, M.A. Alam, I. Wilkinson, R.J. Hughes, I.R. Fisher, P.C. Canfield, T. Jarlborg and G. Santi: Phys. Rev. Lett. **83** (1999) 4824.
- [14] H. Michor, T. Holubar, C. Ducek and G. Hilscher: Phys. Rev. B **52** (1995) 16165.
- [15] S. Manalo, H. Michor, M. El-Hagary and G. Hilscher: Phys. Rev. B **63** (2001) 104508.
- [16] P. Martinez-Samper, H. Suderow, S. Vieira, J. P. Brison, N. Luchier, P. Lejay, P. C. Canfield, S. Manalo, H. Michor, M. El-Hagary and G. Hilscher: Phys. Rev. B **67** (2003) 014526.
- [17] S. V. Shulga, S.-L. Drechsler, G. Fuchs, K.-H. Muller, K. Winzer, M. Heinecke and K. Krug, Phys. Rev. Lett. **80** (1998) 1730.

[18] K. Yamauchi, H. Katayama-Yoshida, A. Yanase and H. Harima: proceedings for ISS 2003, to be published in *Physica C*.

[19] C. Stassis, M. Bullock, J. Zarestky, P. Canfield, A.I. Goldman, G. Shirane and S.M. Shapiro: *Phys. Rev. B* **55** (1997) R8678; H. Kawano, H. Yoshizawa, H. Takeya, and K. Kadowaki: *Phys. Rev. Lett.* **77** (1996) 4628; P. Dervenagias, M. Bullock, J. Zarestky, P. Canfield, B.K. Cho, B. Harmon, A.I. Goldman, and C. Stassis: *Phys. Rev. B* **52** (1995) R9839.

[20] H. Fukazawa, T. Nomura, H. Ikeda and K. Yamada: *J. Phys. Soc. Jpn* **70** (2001) 3011.

[21] W.L. McMillan: *Phys. Rev.* **167** (1968) 331.

[22] N. E. Bickers and S. R. White: *Phys. Rev. B* **43** (1991) 8044.

[23] P. Monthoux and D. Pines: *Phys. Rev. B* **47** (1993) 6069.

[24] H. Kontani, K. Kanki and K. Ueda *Phys. Rev. B* **59** (1999) 14723.

[25] J.R. Schrieffer: *Theory of Superconductivity* (Addison-Wesley Publishing Company, 1998)

[26] P.B. Allen and B. Mitrovic: *Solid State Physics* **37**

[27] Q. Yuan, H.Y. Chen, H. Won, S. Lee, K. Maki, P. Thalmeier and C.S. Ting: *cond-mat/0306293*.

[28] H. Fukazawa and K. Yamada: *J. Phys. Soc. Jpn.* **72** (2003) 2449.

[29] R. Arita, K. Kuroki, and H. Aoki: *Phys. Rev. B* **60** (1999) 14585.

[30] S. Namikawa, T. Moriya and K. Ueda: *J. Phys. Soc. Jpn.* **65** (1996) 4026.

[31] P. Monthoux and G.G. Lonzarich: *Phys. Rev. B* **63** (2001) 054529.

[32] H. Kontani: in preparation.

[33] Y. Yanase, T. Jujo, T. Nomura, H. Ikeda, T. Hotta and K. Yamada: *Phys. Rep.* **387** (2003) 1.

[34] T. Nomura and K. Yamada: *J. Phys. Soc. Jpn.* **71** (2002) 404; T. Noamura and K. Yamada: *J. Phys. Soc. Jpn.* **72** (2003) 2053.

[35] K. Deguchi, Z. Q. Mao, H. Yaguchi and Y. Maeno: *cond-mat/0311366*.

[36] M. B. Maple, P.-C. Ho, N.A. Frederick, V.S. Zapf, W.M. Yuhasz, and E.D. Bauer: *Acta Physica Polonica B* **34** (2003) 919.

[37] H. Kotegawa, M. Yogi, Y. Imamura, Y. Kawasaki, G.-q. Zheng, Y. Kitaoka, S. Ohsaki, H. Sugawara, Y. Aoki, and H. Sato: *Phys. Rev. Lett.* **90** (2003) 027001.

[38] Y. Aoki, A. Tsuchiya, T. Kanayama, S. R. Saha, H. Sugawara, H. Sato, W. Higemoto, A. Koda, K. Ohishi, K. Nishiyama and R. Kadono: *Phys. Rev. Lett.* **91** (2003) 067003.

[39] M. Kohgi: Autumn Meeting of Physical Society of Japan (2003).

[40] J. Goryo: *Phys. Rev. B* **67** (2003) 184511.

[41] K. Izawa, Y. Nakajima, J. Goryo, Y. Matsuda, S. Osaki, H. Sugawara, H. Sato, P. Thalmeier, and K. Maki *Phys. Rev. Lett.* **90** (2003) 117001.

[42] T. Waki, C. Michioka, M. Kato, K. Yoshimura, K. Takada, H. Sakurai, E.T-Muromachi, T. Sasaki: *cond-mat/0306036*; K. Ishida, Y. Ihara, Y. Maeno, C. Michioka, M. Kato, K. Yoshimura, K. Takada, T. Sasaki, H. Sakurai, E.T-Muromachi: *cond-mat/0308506*.

[43] T. Fujimoto, G.-q. Zheng, Y. Kitaoka, R.L. Meng, J. Cmaidalka, C.W. Chu: *cond-mat/0307127*.

[44] Y. Kobayashi, M. Yokoi and M. Sato: *J. Phys. Soc. Jpn.* **72** (2003) 2161; Y. Kobayashi, M. Yokoi and M. Sato: *J. Phys. Soc. Jpn.* **72** (2003) 2453.

[45] K.K. Ng and M. Sigrist: *Europhys. Lett.* **49** (2000) 403; Y. Tanase and M. Ogata: *J. Phys. Soc. Jpn.* **72** (2003) 673.

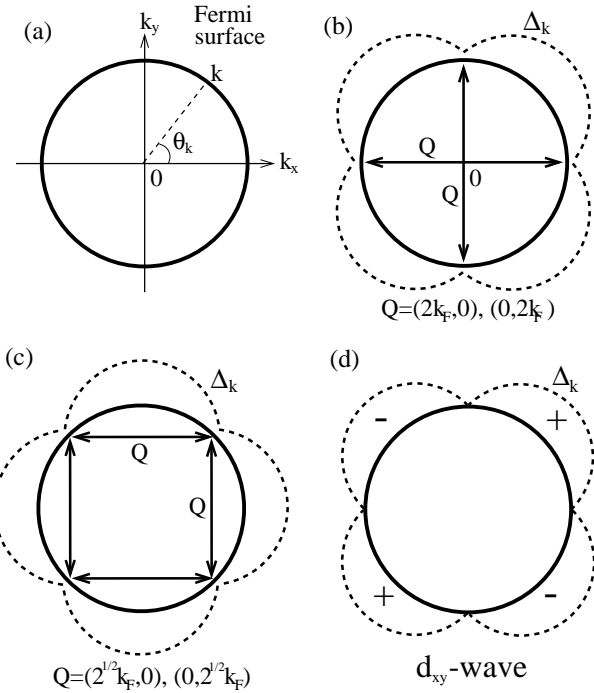


FIG. 1. (a) Fermi surface of the present study. We put  $k_F = \pi/2$ , which corresponds to the quarter-filled band in a square lattice system. (b) anisotropic s-wave SC gap in the presence of the AF fluctuations;  $\mathbf{Q} = (2k_F, 0), (0, 2k_F)$ . (c) anisotropic s-wave SC gap in the case of  $\mathbf{Q} = (\sqrt{2}k_F, 0), (0, \sqrt{2}k_F)$ . (d)  $d_{xy}$ -wave SC gap caused by the AF fluctuations;  $\mathbf{Q} = (Q, 0), (0, Q)$ .

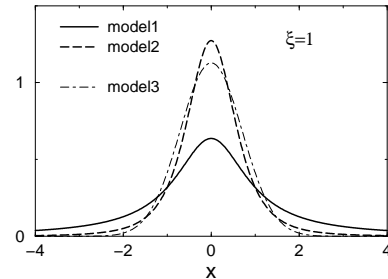


FIG. 2.  $V_{x+Q}^{AF}(0)$  for model 1 and model 2, with  $a = 1$  and  $\xi_{AF} = 1$ . Model 3 is defined as  $V_{x+Q}^{AF}(0) = \sqrt{\pi}a \cdot \exp(-\xi_{AF}^2|x|^2)$ .

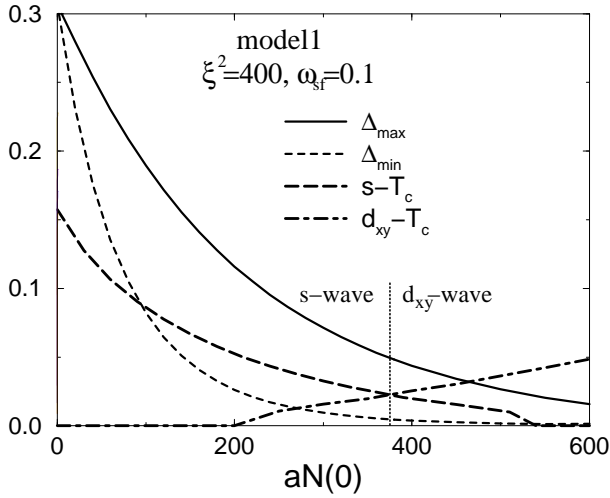


FIG. 3.  $\Delta_{\min,\max}$  and s,d- $T_c$  obtained in model 1 as a function of  $aN(0)$ .

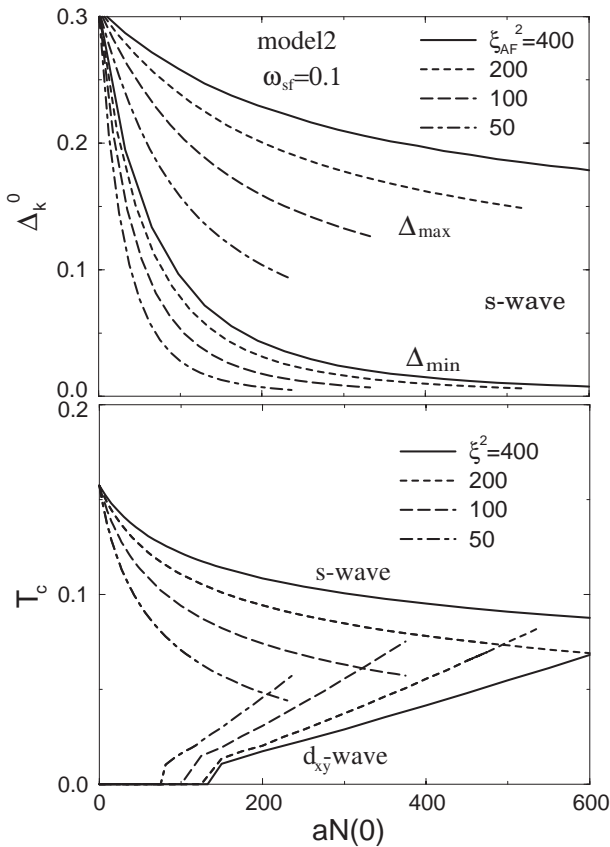


FIG. 4.  $\Delta_{\min,\max}^0$  and s,d- $T_c$  obtained in model 2 for  $\omega_{sf} = 0.1$ .

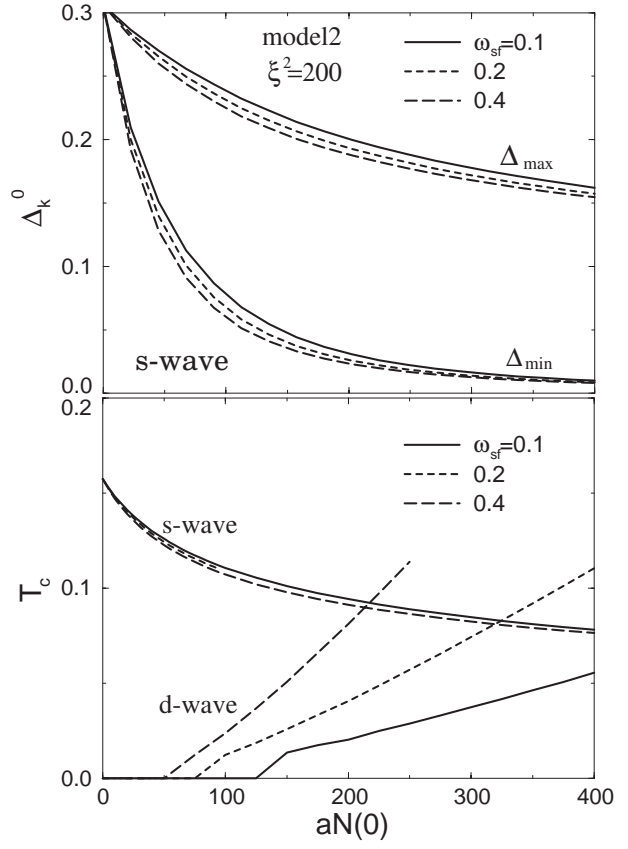


FIG. 5.  $\Delta_{\min,\max}^0$  and s,d- $T_c$  obtained in model 2 for  $\xi_{AF}^2 = 200$ .

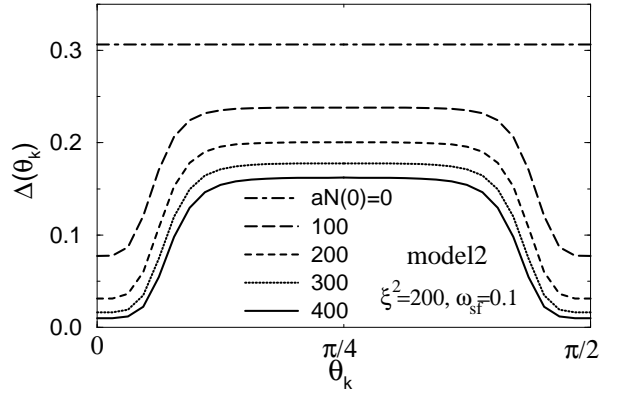


FIG. 6.  $\theta_k$ -dependence of  $\Delta_k^0$  obtained in model 2.

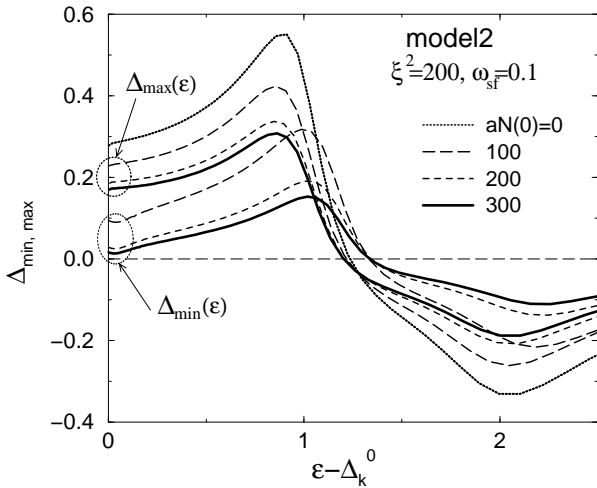


FIG. 7.  $\epsilon$ -dependence of  $\Delta_{\min,\max}(\epsilon)$  obtained in model 2. Here we put  $\Gamma = \omega_{\text{sf}}/6$ .

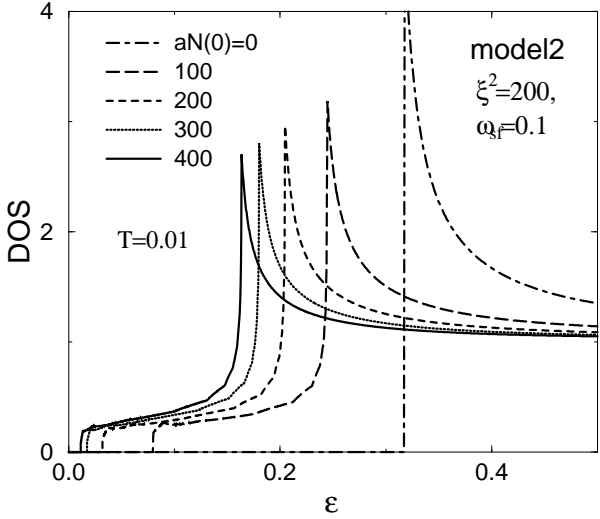


FIG. 8.  $\epsilon$ -dependence of  $\rho(\epsilon)$  obtained in model 2. We put  $N(0) = 1$ .

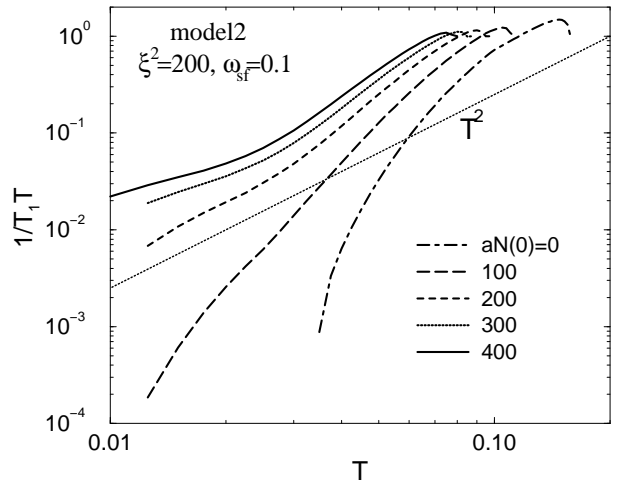
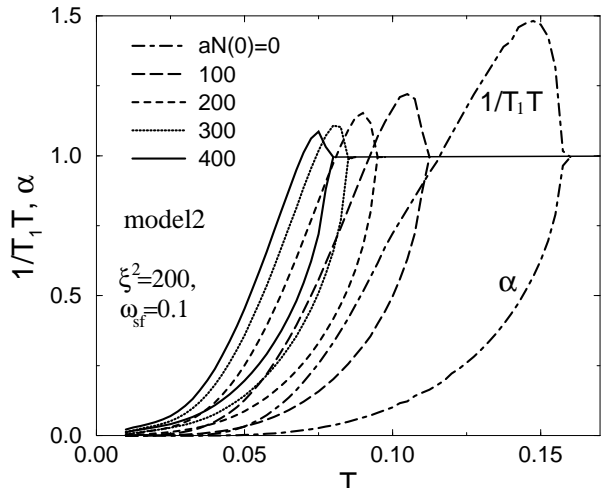


FIG. 9. (a) Obtained nuclear-lattice relaxation ratio  $1/T_1 T$  and ultrasonic attenuation ratio  $\alpha$ . (b)  $1/T_1$  is proportional to  $T^3$  at lower temperatures for  $aN(0) > 200$ , reflecting the deep minima in SC gap.  $1/T_1 \propto T^5$  should be observed in a three-dimensional model.

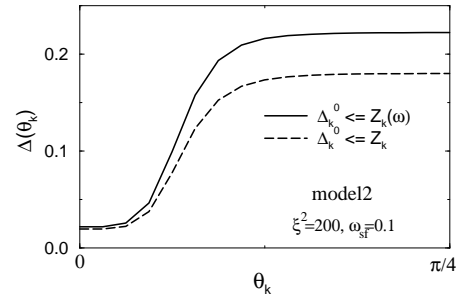


FIG. 10.  $\theta_{\mathbf{k}}$ -dependence of  $\Delta_{\mathbf{k}}^0$  obtained by solving Eliashberg equation when  $aN(0) = 300$ , (i) by dropping the energy-dependence of  $Z_{\mathbf{k}}$  (dashed line) and (ii) by taking the energy-dependence of  $Z_{\mathbf{k}}(\omega)$  into account correctly (full line).

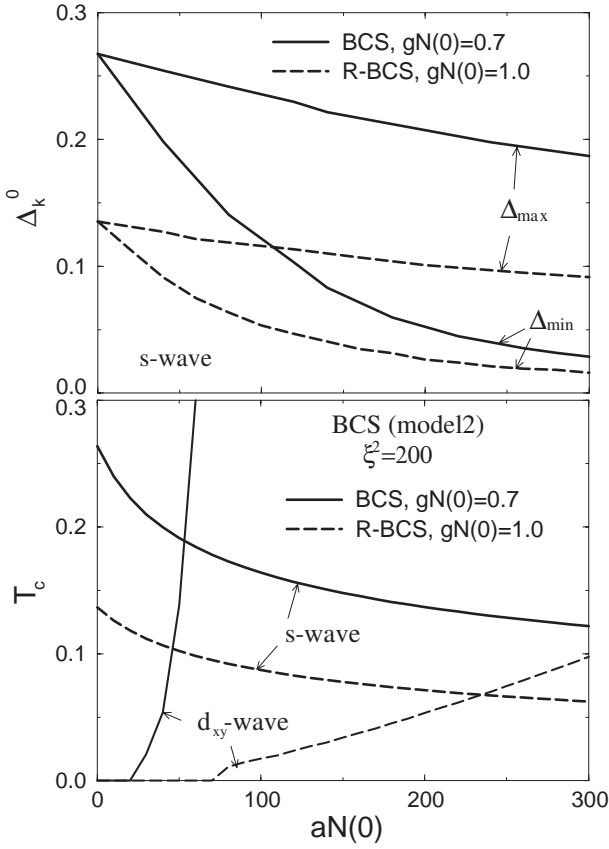


FIG. 11. Obtained  $\Delta_k^0$  and s,d- $T_c$  by BCS theory ( $Z_k = 1$ ) and by R-BCS theory ( $Z_k > 1$ ), respectively.

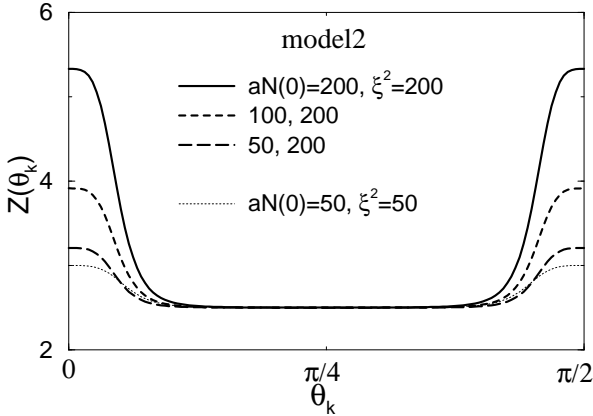


FIG. 12.  $\theta_k$ -dependence of  $Z_k$  for  $\lambda = 1.5$ .

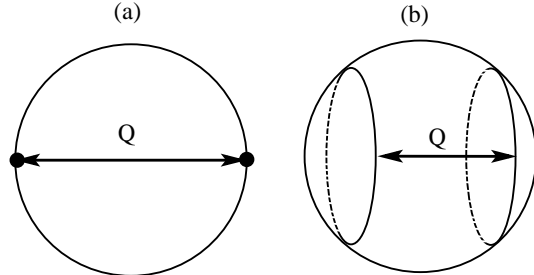


FIG. 13. Illustration of the location of the gap minima for (a)  $|\mathbf{Q}| = 2k_F$  and (b)  $|\mathbf{Q}| < 2k_F$  ( $\mathbf{B} \parallel \hat{x}$ ), in the case of the spherical FS.

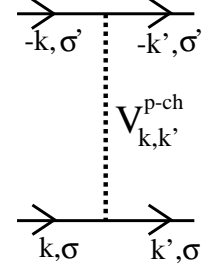


FIG. 14. Paring interaction for the p-wave channel.

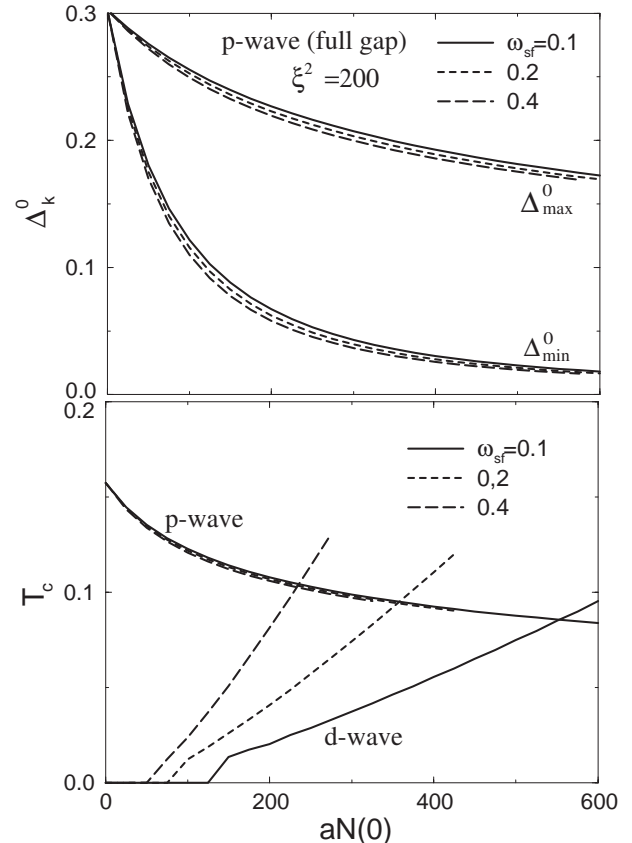


FIG. 15. Obtained quasiparticle gap function  $\Delta_k^0$  for the full-gap p-wave SC state and  $T_c$ 's for both p- and d-wave solutions, as functions of  $aN(0)$ .